Photocatalytic degradation of organic pollutant aldicarb by non-metal-doped nanotitania: synthesis and characterization

Rajesh Kattiparambil Manoharan & Sugunan Sankaran

Environmental Science and Pollution Research

ISSN 0944-1344
Volume 25
Number 21

Environ Sci Pollut Res (2018)
25:20510-20517
DOI 10.1007/s11356-017-0350-2

Springer

Environ Sci Pollut Res (2018) 25:20510–20517
DOI 10.1007/s11356-017-0350-2

Photocatalytic degradation of organic pollutant aldicarb by non-metal-doped nanotitania: synthesis and characterization

Rajesh Kattiparambil Manoharan[1] · **Sugunan Sankaran**[2]

Received: 22 March 2017 / Accepted: 26 September 2017 / Published online: 23 October 2017

Abstract The current study focused on pollution control by titania through photocatalytic degradation of aldicarb pesticide in aqueous medium. Titania, which is an efficient photocatalyst, can bring about degradation of aqueous organic pollutants under UV and visible light irradiation. Here, we prepared titania by sol-gel method from titanium tetraisopropoxide and doped non-metals like N and S from sources such as urea and thiourea, respectively. The prepared catalyst was characterized by XRD, UV-Vis.DRS, TEM, XPS, etc. Photocatalytic activity of the catalyst was evaluated from extend of degradation of aldicarb pesticide by measuring its concentration with the help of HPLC. It was found that the modified catalyst showed better photocatalytic degradation than pure titania in visible light.

Keywords Photocatalysis · TiO_2 · NS co-doped · Aldicarb · Organic pollutant

Introduction

Aldicarb [2-methyl-2-(methylthio)propionaldehyde O-(methylcarbamoyl)oxime] is an extremely toxic systemic carbamate pesticide used in chemical weapon and crop production. Aldicarb derivatives like aldicarb sulphoxides and sulphones that are obtained by the oxidation of aldicarb can enhance crop production but will persist in soil with toxicity similar to that of parent aldicarb (Union Carbide 1983; Suett and Jukes 1988). The half live of aldicarb and its metabolites which are in the range of 29 to 78 days indicate that their decomposition is a very slow process (Chris et al. 2004; Lawrence et al. 2005). Due to the agricultural runoffs, these persist organic pollutants cause contamination even in drinking water (Zaki and Harris 1982; Miles 1991). Hence, its removal or detoxification receives increased importance in current environmental protection (Turan et al. 2008).

There are several pathways such as oxidation, ozonization, hydrolysis, bio microbial, and photolysis which cause degradation of aldicarb and its metabolites in soil thereby generating many toxic by products (Andreozzi et al. 1999; Arancibia et al. 2002; Bandala et al. 2002; Burrows et al. 2002; Neyens and Baeyens 2003; Ikehata and El-Din 2006; Bandala and Estrada 2007; Martínez-Huitle et al. 2008; Tomašević et al. 2010). Also these aqueous persist organic pollutants are resistant to biodegradation and photolytic degradation due to their stable chemical structure (Kexin et al. 2013). Hence, innovation of a prompt method for degradation of these aqueous persistent organic pollutants was a still challenging topic. In this context, photocatalysis was proved to be a remedy (Burrows et al. 2002; Vivechana et al. 2009; Kexin et al. 2013) since such pollutants can be completely degraded to minerals such as carbon dioxide, water, and inorganic substance.

Titanium dioxide is a well-known photocatalyst for the removal or degradation of organic pollutants due to its high chemical stability, strong photo-oxidizing potential, non-toxicity, and low cost (Fujishima and Honda 1972; Wu et al. 2005; Galindo et al. 2008). However, its activity was limited to UV region of the solar source due to its wide band gap of 3.2 eV, (anatase). Many attempts were reported by various

Responsible editor: Suresh Pillai

✉ Rajesh Kattiparambil Manoharan
rajeshkmamangalam@gmail.com

[1] Department of Chemistry, MPMM SN Trusts College, Shoranur, Kerala 679122, India

[2] Department of Applied Chemistry, Cochin University of Science and Technology, Cochin, Kerala 682022, India

research groups to bring the activity of titania into the visible region by doping with metals, non-metals, coupling with other semiconductors, sensitizing titania with other colorful inorganic or organic compounds. Undeniably, the non-metal-doped TiO_2 photocatalyst is a hot research topic, and it opens up a new possibility for the development of solar light-induced photocatytic materials by co-doping with double non-metal.

In addition, rare reports were available regarding high-percentage photocatalytic degradation of aqueous solution of organic pollutant aldicarb in visible light irradiation with non-metal-doped titania. Kexin et al. (2013) reported around 36.8% degradation of 10.5 mg/L of aldicarb solution for 10-h irradiation in visible light; Dong et al. (2012) reported around 60% degradation of 2 mM solution for 3 h irradiation in UV light. So in the present work, we aimed a simple route for synthesis of high visible light responsive N-doped and NS co-doped titania through sol-gel method. The catalyst is characterized by techniques such as XRD, UV-Vis.DRS, TEM, and XPS. The photocatalytic ability of the prepared samples evaluated by studying the photocatalytic degradation of aldicarb pollutants in visible and UV region. The results are compared with pure titania prepared in the same manner and also with the commercially available anatase titania.

Experimental section

Catalyst preparation

(i) Preparation of nitrogen-doped catalyst (N-TiO_2): Take 1:10 ml volume ratio of titanium tetraisopropoxide in isopropyl alcohol. To this, add an aqueous solution of 10% urea in drops. It was stirred mechanically for 12 h. The resulting gel was aged for 1 day, dried at temperature below 70 °C, and calcined at 400 °C for 4 h. (ii) Preparation of nitrogen sulfur co-doped catalyst (NS-TiO_2): The experimental conditions are same as that of the above one. However, the dopant used in this case is 1% aqueous solution thiourea. (iii) Preparation pure titania (L-TiO_2): The experimental conditions are also same as that of the above except the addition of which is pure aqueous solution in this case. (iv) Commercial titania (A-TiO_2): A 100% anatase titania purchased from Sigma Aldrich.

Characterization

The X-ray diffraction (XRD) patterns were recorded using *Bruker* AXS D8 advance X-ray Diffractometer with Ni-filtered Cu Kα radiation (λ = 0.15406 nm). The intensities obtained in the 2θ range 10–70°. The crystallite size was determined from the broadening of the major peak in the XRD spectrum using the Scherrer equation. $D = K\lambda/\beta \cos\theta$, where D is the crystallite size, K = 0.9 is a constant, λ is the X-ray wavelength, β is full width half maximum of the major peak, and θ is the diffraction angle. The UV-Visible diffuse reflectance spectra (UV-Vis.DRS) are recorded in the range of 200–900 nm on a *Labomed* UVD–500 UV-Visible Double beam spectrophotometer equipped with an integrating sphere assembly, using $BaSO_4$ as reflectance standard. The BET surface area was measured using Micromeritics Tristar 3000 surface area and porosity analyzer. The samples were activated at 90 °C for 30 min and degassed at 350 °C for 4 h under nitrogen flow. The transmission electron microscopy (TEM) images were recorded *Jeol* 3010 ultrahigh resolution analytical electron microscope. A sonicated solution of the sample in alcohol, which evaporates on the TEM grid to form a dry film, was prepared. The X-ray photoelectron Spectra (XPS) recorded in an indigenously developed electron spectrometer equipped with *Thermo* VG Clamp-2 Analyser and Mg Kα X-ray source (1253.6 eV, 30 mA × 8 kV). A thin sample wafer of 12 mm in diameter was used in these studies. Absolute binding energy of C 1*s* peak at 284.6 eV was used as an internal reference.

Photocatalytic activity

The experiments were carried in Oriel Arc lamp system designed to produce uniform illumination (Oriel Uniform Illuminator). This system delivers a 1.0-in. (2.54 cm) diameter collimated beam. The work plane is 2.6 in. (6.65 cm) from the bottom of the beam turning assembly. Uniform illuminator contains a fan-cooled lamp housing that offers a temperature-controlled, stable environment for the lamp. The light source used in this system is 100 W Xe ozone free lamps with an average life of 500 h. The various filters used in this system are (i) 280–400-nm dichroic mirror with irradiance of 29.9 mW/cm^2 for UV irradiation and (ii) 420–630-nm dichroic mirror (cold mirror) with irradiance of 64.7 mW/cm^2 for visible irradiation.

Studies involve a 10 ml of 10^{-4} M aqueous solution of Aldicarb taken in beaker placed below the beam turning assembly unit, which holds the dichroic mirrors under room temperature. The mixture was stirred for 30 min to achieve the adsorption equilibrium before the lamp was turned on for the photocatalytic reaction to begin. After the irradiation, the solution was taken out from the light source and centrifuged to remove the catalyst particles. The solution is properly diluted to measure its concentrations using HPLC (Dionex Ultimate 3000) with photo diode array UV detector and a 5-μm Thermo Hypersil ODS-2 C-18 reverse phase column (150 × 4.6 mm) with mobile phase of acetonitrile/water in the ratio of 30:70 (1.0 ml/min) and UV detection at 246 nm. The percent of degradation was calculated as follows: Percent of Degradation = {Co − C} × 100/Co, where Co and C are the concentration of sample before and after irradiation.

Studies such as the change in amount of catalyst, comparison of percent degradation in visible and UV region, and adsorption were conducted.

Results and discussion

Catalyst preparation

In sol-gel method, the morphological properties of the catalyst are controlled by the addition of acids or bases, which depends on the point of zero charge of the particles (Leticia et al. 2013; Rajesh and Sugunan 2012). In the present study, we introduced an aqueous solution of dopant and avoided the addition of any acid or bases. The addition of aqueous medium facilitates the easy precipitation of the catalyst and reduces its activities. The introduction of strong mechanicals stirring helps to avoid such precipitation process and that controls the morphological properties through formation of the sol. The sol formation permits the formation of fine particles, prevents the degree of agglomeration, and limits the particle-particle interaction. In our study, we optimized the stirring time of 12 h. The increase in the time of stirring results in the instability of dopant speicies. As the stability of dopant species decreases, it decreases the activity of the modified catalysts in visible light irradiation.

X-ray diffraction

Figure 1 shows the XRD spectra. All the samples showed a major peak at 2θ of 25.4°, which is the characteristic of (101) plane of anatase phase. The absence of other major peaks confirmed the presence of anatase phase only. All catalysts showed more or less equal d spacing value (for the major peak) which indicated the stabilization of anatase phase by the dopant. The slight changes may be due to the lattice expansion along c-axis because of anion incorporation (Lin et al. 2007). The average crystallite size was calculated from the broadening of (101) XRD peaks of anatase using the Scherrer equation around 10 nm for doped catalysts. The broadening of the peaks in the prepared samples indicated that the particle size has decreased compared to commercial sample (Reddy et al. 2005; Qin et al. 2008; Sathish et al. 2005; Hexing et al. 2006; Rajesh and Sugunan 2012). Peaks due to the dopants were absent. This revealed that the structure of titania is not affected by the incorporation of the dopants.

UV-Visible diffuse reflectance spectra

Figure 2 shows the UV-Visible diffuse reflectance spectra. The absorption edges obtained as the wavelength of the onset of the spectrum are converted to bandgap (Yin et al. 2007) using one of the forms of Kubelka-Munk function (Eg = 1239.8/λ). Incorporation of dopants N and S are indicated by the color change of the samples from white to pale yellow. The doped samples showed a red shift in absorption maximum and possessed two absorption edges compared to pure titania. The absorption edges were related to original structure and doped structure of titania (Yin et al. 2006; Rajesh and Sugunan 2012). The red shift was due to the impurities incorporated into titania framework, which resulted in narrowing the bandgap by mixing their p states with O 2p orbitals.

Specific surface area (BET)

The specific surface areas of NS-TiO_2, N-TiO_2, and L-TiO_2 are 122.9, 100.9, and 85.7 m^2/g, respectively. The results indicated the successive incorporation of dopant in the titania lattice. It was already mentioned by many authors that the advantages of the preparation of doped titania by the sol-gel method is that the specific surface areas can be increased depending on the nature of the doping agent (Gomez et al. 2003; Galindo et al. 2008). They suggested that the presence of dopant disturb the hydrolysis-condensation reactions of the titanium alkoxide, results in the increase of specific surface area. The actual mechanism by which the increase of surface

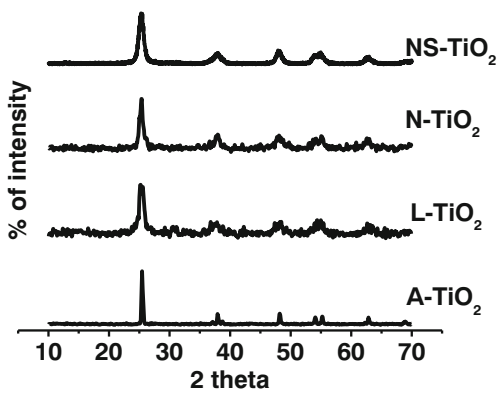

Fig. 1 XRD spectra of A-TiO_2, L-TiO_2, N-TiO_2, and NS-TiO_2

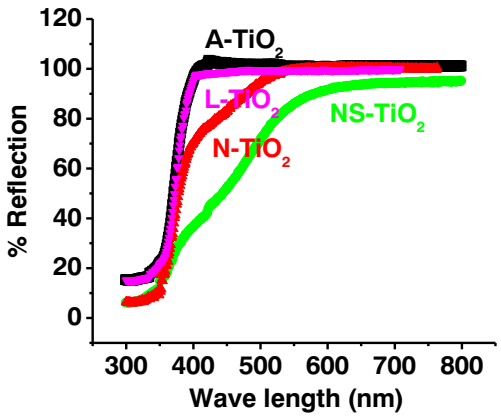

Fig. 2 UV-Vis.DRS spectra of A-TiO_2, L-TiO_2, N-TiO_2, and NS-TiO_2

area is not well established, and however, we suggested that it may be due to the substitution of Ti or and O in the titania lattice by the dopant elements.

Transmission electron microscopy studies

Figure 3a–f shows the TEM, selected area electron diffraction (SAED), and high-resolution TEM images of catalyst N-TiO_2 and NS-TiO_2. The TEM images showed that particle size of NS-TiO_2 and N-TiO_2 is in the range 7–13 nm. From the HRTEM and SAED, the *d* value corresponding to the (101) plane of the anatase phase was calculated. The particle size and anatase (101) plane obtained from the TEM study showed very good agreement with that obtained from XRD. The powders found to be fine and slightly agglomerated.

X-ray photoelectron spectra studies

The XPS data are presented in Fig. 4a–g and atomic concentration values derived from the XPS data are presented in Table 1. For oxygen, the 1*s* XPS spectra was de-convoluted using Gaussian multi-peak fitting program and peak area at 529.3 eV was taken for atomic ratio calculation purpose. Areas for corresponding peaks were divided by the sensitivity factors in these calculations. At some places, C 1*s* peak with binding energy value of 284.8 eV was referred as standard value for the surface adventitious carbon. Thus, if we include this correction, the B.E. values observed in present study will be shifted to higher side by 0.2 eV.

The Ti 2*p* XPS spectra showed two peaks, one at 458.2 and other at 464.7 eV in the case N doping (Fig. 4a) and 458.4 and 464.1 eV in the case of NS co-doping (Fig. 4d). These were assigned to the Ti $2p_{3/2}$ and Ti $2p_{1/2}$ states. These doublet peaks were due to the spin-orbit splitting of Ti 2*p* (Wang et al. 2008). The above value corresponds to (IV) oxidation state of Ti. Thus, in the prepared samples, titanium had (IV) oxidation state with stable Ti–O bond. For the pure titania, these peaks were observed at 458.9 and 464.7 eV, respectively, which were contributions from O-Ti-O in TiO_2 (Sathish et al. 2005; Wong et al. 2006; Rajesh and Sugunan 2012). The binding energy shifts were smaller for the doped samples. These shifts of Ti core level signal, which were attributed to Ti 2*p* peaks of Ti-O-N linkage, suggested the successful incorporation of the dopant into the titania lattice.

The O 1*s* XPS showed a strong peak at 529.3 eV corresponding to bulk oxygen bonded to titanium where as a weak shoulder at 531 eV was due to the presence of oxygen attached to N (Fig. 4b). The weak shoulder at higher binding energy was associated with hydroxyl groups adsorbed on the TiO_2 surface. But in the case, NS co-doping (Fig. 4e) showed another weak shoulder at higher binding energy of 532.2 eV which may be due to the incorporation of S as SO_4^{2-} (Rajesh and Sugunan 2012).

The S 2*p* XPS spectrum (Fig. 4g) showed a peak at 168.5 eV corresponding S $2p_{3/2}$ state. Peak of S 2*p* at 168.0–170.0 eV corresponds to the S atom incorporated as cation in the form of S (VI) in titania network and peak at 160.0–163.5 eV corresponds to S atom as S^{2-} by anionic replacement of O from titania lattice (Ohno et al. 2008; Wang et al. 2008; Rajesh and Sugunan 2012). Thus, the results indicated S in S (VI) state (as SO_4^{2-}). These sulfate ions can form S=O and S–O–S bonds on the TiO_2 surface, creating unbalanced charge on Ti and vacancies/defects in the titania network.

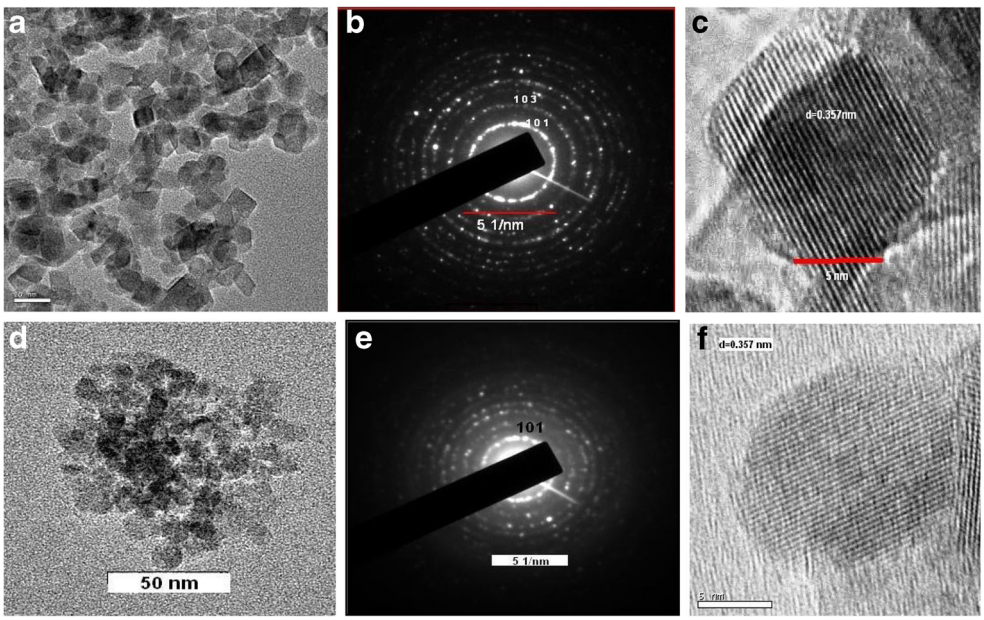

Fig. 3 **a** TEM, **b** SAED, **c** HRTEM of N-TiO_2, **d** TEM, **e** SAED, and **f** HRTEM of NS-TiO_2

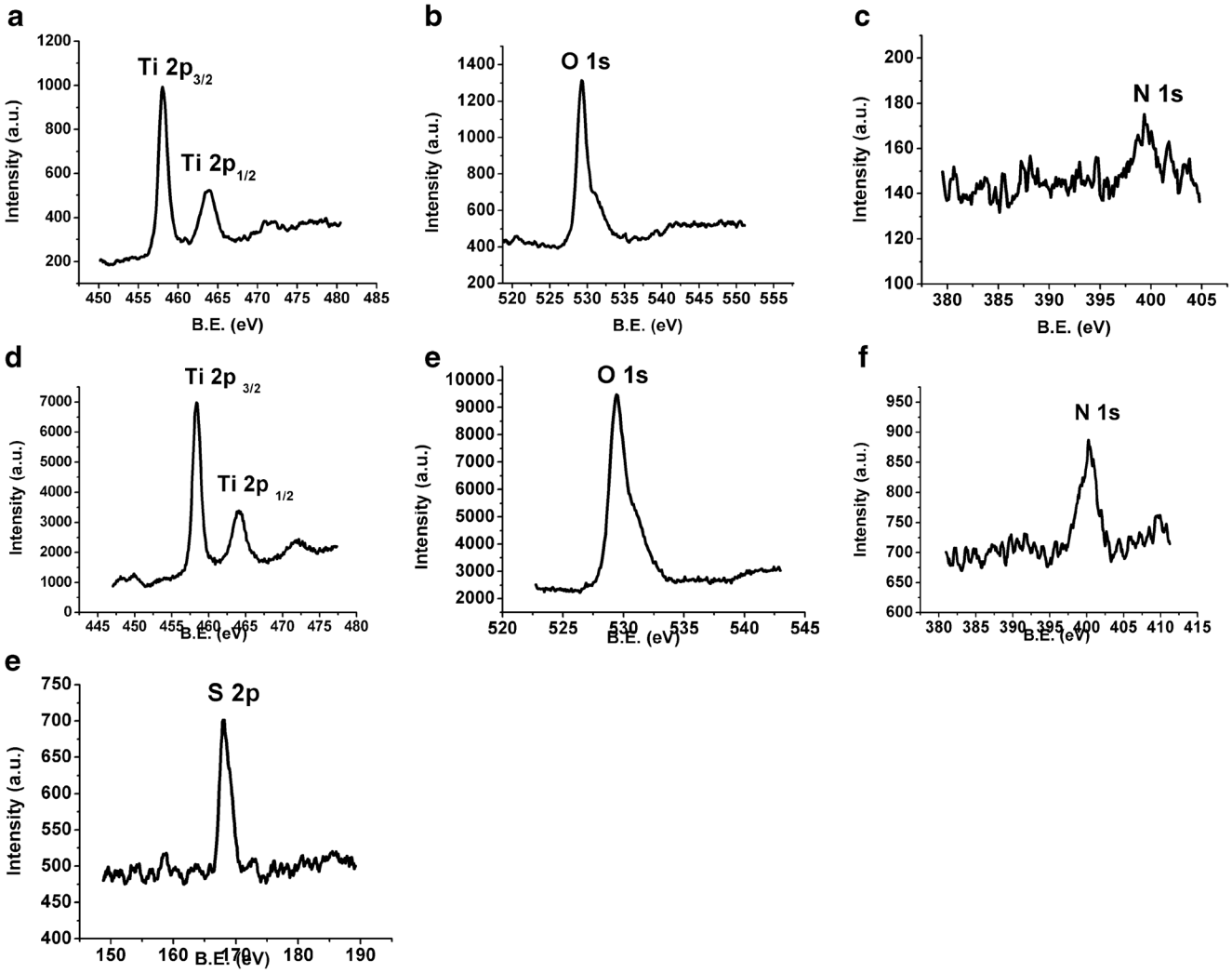

Fig. 4 **a** Ti 2*p* XPS spectra of N-TiO2. **b** O 1*s* XPS spectra of N-TiO2. **c** N 1*s* XPS spectra of N-TiO2. **d** Ti 2*p* XPS spectra of NS-TiO2. **e** O 1*s* XPS spectra of NS-TiO2. **f** N 1*s* XPS spectra of NS-TiO2. **g** S 2*p* XPS spectra of NS-TiO2

The N 1*s* XPS spectrum showed a peak at 399.5 eV corresponding to the N doping (Fig. 4c) and peak at 400.2 eV corresponding to the NS co-doping (Fig. 4f) catalysts. The assignment of the XPS peak of N 1*s* has still been under debate. The controversial hypotheses have been provided, since the preparation methods, conditions, and source of dopant largely affect N XPS spectral features (Sathish et al. 2005; Xiaobo and Clemens 2004; Wong et al. 2006; Sakthivel et al. 2004; Tingli et al. 2005; Cong et al. 2007; Shen et al. 2008; Feng et al. 2008; Kisch et al. 2007; Rajesh and Sugunan 2012). Thus, our results indicate a peak at 399.5 eV of N doping catalyst which can be assigned to the interstitial N bounded to one lattice oxygen as Ti-O-N. The peak at 400.2 eV of NS co-doping system was due to the presence of incorporated S atom in the lattice. The shift of binding energy to higher values indicated a decrease in the electron density of N atom. We propose that the positive shift of binding energy of N 1*s* in NS co-doping system could be due to the presence of S incorporated as S (VI) assigned to the SO_4^{2-} adsorbed on the surface.

Photocatalytic activity

Effect of catalyst amount

Photocatalytic degradation of aldicarb against the amount of catalyst is shown in Fig. 5a. A 10 ml of 10^{-4} M aqueous solution of aldicarb and catalyst amount of 1.0 to 2.0 g/L with an increment of 0.5 g and a dichroic mirror with 420–630 nm was used for the source visible light are taken for this study. From the results, it is clear that the photocatalytic degradation increases with increase of catalyst amount and reaches an optimum value. The optimum value in this case is 1.5 g/L. The increase of photocatalytic activity with increase of catalyst amount is assigned to the increase of active surface for the formation of activated photo-excited species.

Table 1 Atomic ratios derived from XPS data

XPS of atoms	Parameters	Catalysts	
		N-TiO_2	NS-TiO_2
Ti $2p_{3/2}$ peak (5.22)[a]	B.E. (eV)	458.2	458.4
	FWHM (eV)	1.07	1.13
	Peak area	977.9	7194.8
O 1*s* peak (2.85)[a]	B.E. (eV)	529.2	529.4
	FWHM (eV)	1.07	1.05
	Peak area	961.9	7069.2
N 1*s* peak (1.74)[a]	B.E. (eV)	399.5	400.3
	FWHM (eV)	3.0	2.41
	Peak area	89.3	485.9
S 2*p* peak (1.25)[a]	B.E. (eV)		168.3
	FWHM (eV)		1.70
	Peak area		435
	Ti:O:N		1:1.80:0.27
	Ti:O:N:S		1:1.86:0.09:0.18

This optimum limit depends on the geometry and working conditions of the photo reactor and for a definite amount of catalyst in which all the particles, i.e., surface exposed are very illuminated. When the catalyst concentration increases beyond the optimum value, it causes turbidity in solution. This turbidity prevents the penetration of light to the catalyst surface. Thus, in any given application, the optimum catalyst concentration must be determined, in order to avoid excess catalyst and ensure total absorption of efficient photons.

Effect of time

Add 1.5 g/L of the catalyst to 60 ml of 10^{-4} M aqueous solution of aldicarb and a dichroic mirror with 420–630 nm was used for the source visible light. After the lamp was switched on, around 10 ml of the suspension was pipetted out from the solution at an interval of 7 min each up to 35 min and analyzed using HPLC. Figure 5b shows the percent degradation of aldicarb against time. The result showed a linear relationship with percent degradation and time, i.e., the percent of degradation increases with increase in the irradiation time. As time of irradiation increases, more and more light energy falls on the catalyst surface, which increases the formation of photo-excited species and thereby enhances the photocatalytic activity.

Effect of light source

Studies involve the usage of 10 ml 10^{-4} M aqueous solution of aldicarb with a catalyst amount of 1.5 g/L and light illumination of 30 min. The dichroic mirror of 280–400 and 420–630 nm was used for the source of UV light and visible light, respectively. Blank experiment was conducted without using catalyst in visible light and an experiment without light source. Study involves a comparison of the percent of degradation of both modified catalysts with pure titania prepared in our laboratory and commercially available 100% anatase titania in UV, visible light irradiation, and adsorption.

Table 2 represents the percent of degradation of aldicarb against both the modified and pure titania in UV and visible light irradiation. Results show that both the modified catalysts give better activity for the degradation of aldicarb in visible light irradiation when compared with pure and commercial titania whereas activity decreased in UV light irradiation. The adsorption studies show that the commercial anatase sample gives very good adsorption relationship with the aldicarb. The higher activity of modified catalysts in visible light is attributed to the presence of dopant elements. The dopants could lower the band gap of titania by the presence of an impurity state on the upper edge of the valence band. Thus, mixing the N 2*p* and/or S 2*p* states with O 2*p* state could narrow the band gap of modified titania powders and can lead

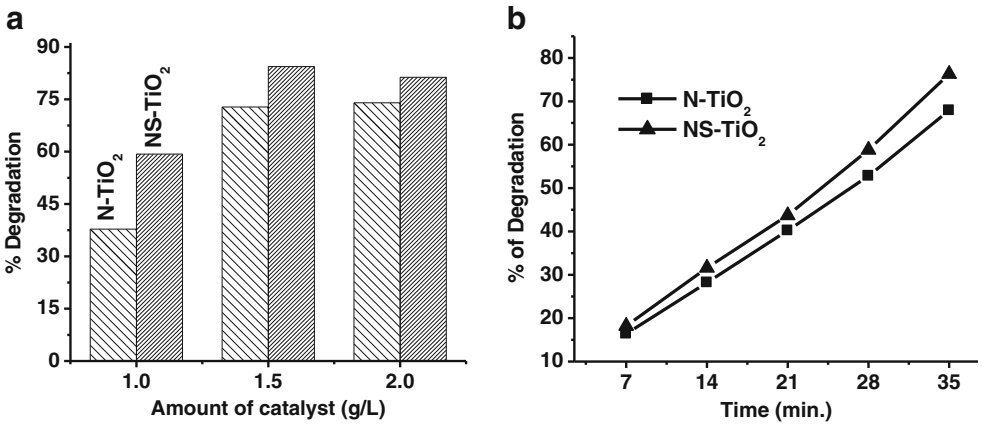

Fig. 5 **a** Percent degradation of aldicarb against amount of catalyst irradiation time: 30 min; aldicarb con. 10 ml of 10^{-4} M. **b** Percent degradation of aldicarb against time amount of catalyst: 1.5 g/L; aldicarb con. 60 ml of 10^{-4} M

Table 2 Percent degradation of aldicarb against light source. (Irradiation time: 30 min.; aldicarb con.: 10 ml of 10^{-4} M; catalyst amount: 1.5 g/L)

Studies	% of degradation				
	N-TiO_2	NS-TiO_2	L-TiO_2	A-TiO_2	Without catalyst
Visible light (420–630 nm)	72.8	84.4	35.9	42.0	8.2
UV light (280–400 nm)	42.0	50.8	72.0	95.6	–
Adsorption	8.9	12.6	11.2	32.2	–

to a stronger absorption in the visible light region. The higher activity of pure and commercial titania in UV irradiation is attributed to its bandgap.

Conclusions

We were successful in synthesizing high visible light responsive anatase NS co-doped and N-doped nanocrystalline titania through sol-gel precipitation method. The mechanical stirring and its duration helps the catalysts with optimized morphological and activity properties. The XRD characterizations showed that particles were crystallite in anatase phase. This was further confirmed by TEM analysis. The particle size (7–13 nm) obtained from TEM showed very good agreement with XRD. The XPS analysis confirmed the incorporation of dopants N and S in titania lattice. The XPS showed the chemical nature of dopant such as N that existed as Ti-O-N and S existed as S (VI) cation. UV-Visible DRS spectrum showed that the absorption edges of doping catalysts shifted to visible region, which lead to narrowing of band gap. The photo catalytic activities of the samples were evaluated by the degradation of the pesticide aldicarb in aqueous solution. It was seen that more than 80% of the pesticide degrade within half an hour irradiation under visible light with 1.5 g/L of NS co-doped catalyst system. This higher activity is due to the synergetic effect of two impurities (both N and S) in their lattice, which brings about reduction of band gap.

Acknowledgements The authors are gratefully acknowledging the financial support given by the Board of Research in Nuclear Science (BRNS) (No. 2006/37/34/BRNS), Department of Atomic Energy (DAE), and Government of India. We are also gratefully acknowledging the analytical facility provided by SAIF, Cochin University of Science and Technology and SAIF, IIT Chennai.

References

Andreozzi R, Caprio V, Insola A, Marotta R (1999) Advanced oxidation processes (AOP) for water purification and recovery. Catal Today 53(1):51–59

Arancibia C, Bandala ER, Estrada C (2002) Radiation absorption and rate constants for carbaryl photocatalytic degradation in a solar collector. Catal Today 76(2):149–159

Bandala ER, Estrada C (2007) Comparison of solar collection geometries for application to photocatalytic degradation of organic contaminants. J Sol Energy Eng 129:22–26

Bandala ER, Gelover S, Leal T, Arancibia C, Jiménez A, Estrada C (2002) Solar photocatalytic degradation of aldrin. Catal Today 76(2):189–199

Burrows HD, Canle ML, Santaballa JA, Steenken S (2002) Reaction pathways and mechanisms of photodegradation of pesticides. J Photochem Photobiol B Biol 67:71–108

Chris WP, Jane FF, Russell LJ (2004) Pulsed losses and degradation of aldicarb in a South Florida Agricultural Watershed. Arch Environ Contam Toxicol 48:24–31

Cong Y, Jinlong Z, Feng C, Masakazu A, Dannong H (2007) Preparation photocatalytic activity and mechanism of nano TiO_2 co-doped with nitrogen and Iron(lll). J Phys Chem C 111(28):10618–10623

Dong JW, Nathaniel SH, Yong LJ, SKay O (2012) Photocatalytic self-detoxification by coaxially electrospun fiber containing titanium dioxide nanoparticles. Text Res J 82(18):1920–1927

Feng P, Lingfeng C, Hao Y, Hongjuan W, Jian Y (2008) Synthesis and characterization of substitutional nitrogen doped titanium dioxides with visible light photocatalytic activity. J Solid State Chem 181(1): 130–136

Fujishima A, Honda K (1972) Electrochemical photolysis of water at a semiconductor electrode. Nature 23:37–38

Galindo F, Gomez R, Aguilar M (2008) Photodegradation of the herbicide 2,4-dichlorophenoxyacetic acid on nanocrystalline TiO_2-CeO_2 sol-gel catalysts. J Mol Catal A Chem 281:119–225

Gomez R, Lopez T, Ortiz-Islas E, Navrrete J, Sanchez E, Tzompantzi F, Bokhimi X (2003) Effect of sulfation on the photoactivity of TiO2 sol–gel derived catalysts. J Mol Catal A Chem 193:217–226

Hexing L, Jingxia L, Yuning H (2006) Highly active TiO_2N photocatalysts prepared by treating TiO_2 precursors in NH_3/ethanol fluid under supercritical conditions. J Phys Chem B 110(4):1559–1565

Ikehata K, El-Din MG (2006) Aqueous pesticide degradation by hydrogen peroxide/ultraviolet irradiation and Fenton type advanced oxidation processes: a review. J Environ Eng Sci 5(2):81–135

Kexin L, Jingjing X, Tong C, Liushui Y, Yuhua D, Dongyang S, Ying L, Zhenxing Z (2013) Preparation of graphen/TiO2 composites by non ionic surfactant strategy and their simulated sunlight and visible light photocatalytic activity towards representative aqueous POPs degradation. J Hazard Mater 250-251:19–28

Kisch H, Sakthivel S, Janczarek M, Mitoraj D (2007) A low-band gap, nitrogen-modified titania visible-light photocatalyst. J Phys Chem C 111(30):11445–11449

Lawrence KS, Yucheng F, Lawrence GW, Burmester CH, Norwood SH (2005) Accelerated degradation of aldicarb and its metabolites in cotton field soils. J Nematol 37(2):190–197

Leticia FV, Marta H, Julien P, Roger G, Vix-G C, Conchi OA (2013) Tuning the photocatalytic activity and optical properties of mesoporous TiO_2 spheres by a carbon scaffold. J Catal 2013:9

Lin L, Zheng RY, Xie JL, Zhu YX, Xie YC (2007) Synthesis and characterisation of phosphor and nitrogen co-doped titania. Appl Catal B Environ 76:196–202

Martínez-Huitle CA, De Battisti A, Ferro S, Reyna S, Cerro M, Quiroz MA (2008) Removal of the methamidophos pesticide from aqueous solution by electrooxidation using Pb/PbO_2, Ti/SnO_2 and Si/BDD electrodes. Environ Sci Technol 42:6929–6935

Miles CJ (1991) Degradation of aldicarb, aldicarb sulfoxide, and aldicarb sulfone in chlorinated water. Environ Sci Technol 25:1774–1779

Neyens E, Baeyens J (2003) A review of classic Fentons peroxidation as an advanced oxidation technique. J Hazard Mater B 98:33–50

Ohno T, Mitsui T, Matsumura M (2008) Photocatalytic activity of S doped TiO_2 ohotocatalyst under visible light. Chem Lett 32(4): 364–365

Qin H-L, Gu G-B, Liu S (2008) Preparation of nitrogen doped titania with visible-light activity and its application. C R Chim 11:95–100

Rajesh KM, Sugunan S (2012) Effect of mechanical stirring on the preparation of high visible light active N S co-doped nano titania: synthesis and characterisation. J Appl Chem 2(2):36–42

Reddy KM, Baruwati B, Jayalakshmi M, MohanRao M, Manorama SV (2005) S-,N- and C doped titanium dioxide nanoparticles: synthesis, characterization and redox charge transfer study. J Solid State Chem 178:3352–3358

Sakthivel S, Janczarek M, Kisch H (2004) Visible light activity and photoelectrochemical properties of nitrogen doped TiO_2. J Phys Chem B 108(50):19384–19387

Sathish M, Viswanathan B, Viswanath RP, Gopinath CS (2005) Synthesis, characterization, electronic structure and photocatalytic activity of nitrogen doped TiO2 nanocatalyst. Chem Mater 17(25): 6349–6353

Shen XZ, Guo J, Liu ZC, Xie SM (2008) Visible light driven titania photocatalyst co-doped with nitrogen and ferrum. Appl Surf Sci 254(15):4726–4731

Suett DL, Jukes AA (1988) Accelerated degradation of aldicarb and its oxidation products in previously treated soils. Crop Prot 7:147–152

Tingli M, Morito A, Eiichi A, Isao I (2005) High- efficiency dye-sensitized solar cell based on a nitrogen doped nanostructured titania electrode. Nano Lett 5(12):2543–2547

Tomašević A, Mijin D, Kiss E (2010) Photochemical behavior of the insecticide methomyl under different conditions. Sep Sci Technol 45(11):1617–1627

Turan K, Levent K, Muhittin S, Songul K, Ahmet A (2008) Bacterial biodegradation of aldicarb and determination of bacterium which has the most biodegradative effect. Turk J Biochem–Turk J Biochem 33(4):209–214

Union Carbide (1983) Temik aldicarb pesticide: a scientific assessment. Union Carbide Agri Pro Com., Research Triangle Park, p 37

Vivechana D, Jagdish CT, Obendrof SK (2009) Identification of degraded products of aldicarb due to the catalytic behaviour of titanium dioxide/polyacrylonitile nano fiber. J Chromatogr A 1216:6394–6399

Wang Y, Wang Y, Meng Y, Ding H, Shan Y, Zhao X, Tang X (2008) A highly efficient visible light activated photocatalyst based on bismuth and sulphur co-doped TiO_2. J Phys Chem C 112(17):6620–6626

Wong MS, Chou HP, Yang TS (2006) Reactively sputtered N-doped titanium oxide films as visible light photocatalyst. Thin Solid Films 494:244–249

Wu PG, Ma CH, Shang JK (2005) Effects of nitrogen doping on optical properties of TiO_2 thin films. Appl Phys A Mater Sci Process 81(7): 1411–1417

Xiaobo C, Clemens B (2004) Photoelectron spectroscopic invesitigation of nitrogen-doped titania nano particles. J Phys Chem B 108:15446–15449

Yin S, Ihara K, Aita Y, Komatsu M, Sato T (2006) Visible-light induced photocatalytic activity of $TiO_{2-x}A_y$(A=N,S) prepared by precipitation route. J Photochem Photobiol A Chem 179:105–114

Yin S, Komatsu M, Zhang Q, Saito F, Sat T (2007) Synthesis of visible-light responsive nitrogen/carbon doped titania photocatalyst by mechanochemical doping. J Mater Sci 42(7):2399–2404

Zaki D, Harris D (1982) Pesticides in groundwater. The aldicarb story in Suffolk County, NY. Am J Public Health 72:1391–1395